A RECONFIGURABLE RADAR FOR ICE AND SNOW MEASUREMENTS ONBOARD ULTRA-LONG ENDURANCE UAS: DEVELOPMENT AND FLIGHT TESTS

Emily Arnold[1], Carl Leuschen[1], Daniel Gomez-Garcia[1], Sam Ross[1], Jilu Li[1], Matthew Turner[1], John Paden[1], John Papapolymerou[2], Cory Hilton[2], Shravan Kaundinya[1], and Fernando Rodriguez-Morales[1]
[1]Center for Remote Sensing and Integrated Systems, University of Kansas, Lawrence, Kansas USA
[2] Michigan State University, East Landing, Michigan USA

ABSTRACT

In this paper we present the design of a reconfigurable radar flight tested on an ultra-long endurance UAS (Unmanned Aerial System). The radar consists of a common digital backend and swappable RF (radio frequency) front ends. Given this development was designed to support ice and snow measurements in polar regions, two RF modules were fabricated and integrated into the system for testing. A low-Very High Frequency (VHF) RF subsystem operating from 60-80 MHz was developed for ice sounding, while a 2-8 GHz subsystem is to support snow thickness and near-surface ice measurements. This paper provides a brief overview of the various radar subsystems, laboratory test results, aircraft integration, and flight-test results.

Index Terms— Ice penetrating radar, snow-probing microwave radar, UAS-borne radar, ice sheets.

1 INTRODUCTION

Unmanned Aerial System (UAS) radars offer new opportunities in the field of airborne remote sensing of snow and ice. While these smaller vehicles have limited payload capacities as compared to manned vehicles, recent miniaturization of radar electronics have made them viable platforms. In light of this, two different avenues are being explored for UAS-based radar measurements in the cryosphere, the first being short range surveys that aim to measure a single target and can be conducted by small research groups, while the second is long-range surveys aimed at addressing the remaining gaps in ice measurements. The latter surveys typically require the involvement of multiple shareholders due to the vehicle cost and complexity.

Short-range surveys are best suited for small- to medium-sized UAS, or Group I and II class vehicles [1], as they can be operated by most individuals with minimal training. The Center for Remote Sensing and Integrated Systems (CReSIS) at the University of Kansas flew Very High Frequency (VHF) radars on both an Aurelia X6 and an AeroVironment Vapor-55. These systems were used to survey the grounding line of Helheim Glacier in Greenland in 2021 [3],[4]. Similarly, the Standford Radio Glaciology Lab, developed a 300-450 MHz ice penetrating radar to survey glaciers in Svalbard [5],[6].

Meanwhile, larger Group 3-5 vehicles are better suited for long-range surveys. Long-endurance UAS such as Global Hawk and Platform Aerospace's Vanilla can fly surveys more than 20 hours long. While range is the key metric in ice and snow surveys rather than endurance, these extreme endurances naturally result in superior survey distances. CReSIS has previously integrated and flown their 2-8 GHz "Snow Radar" on Vanilla UAS. The system flew in 2021 from Deadhorse, Alaska [2] and 2023 from Thule, Greenland for the purpose of measuring snow on sea ice.

This work seeks to expand the UAS-borne radar capabilities of CReSIS through the development of a reconfigurable radar with swappable RF-front ends. The motivation for this work is to create an adaptable radar system that could be flown on a variety of UAS and support a range of science missions and inherently eliminates the need for discrete radar systems for each measurement.

This system was integrated and flight tested on the Vanilla UAS in late 2024. While the radar performance was expected to be comparable to existing technology, the system integrated onto the Vanilla UAS will enable access to highly remote Arctic and Antarctic regions at a much lower cost than manned platforms. While the vehicle has an endurance of four days with maximum payload, the reality is that flights with the Vanilla will be limited by weather. For a two-day weather window, the Vanilla would cover ~4,600 km. Figure 1 shows potential coverage maps for the Antarctic continent and Arctic sea ice. Antarctic missions typically consist of flying to a target and then conducting a gridded survey. In Figure 1a, the circle radii are equivalent to 1,600 km and represent a maximum ingress/egress distance for a survey flight starting from the various stations. For this ingress/egress distance, the Vanilla could conduct a 1,400 km survey. For longer weather windows or shorter surveys (thus longer ingress/egress), it would be possible for Vanilla to reach all regions of the continent from the four stations identified. Lastly, it should be noted that, for the same mission profile indicated in Figure 1a, the Vanilla could survey any point in Greenland regardless of where it is launched within the country.

In the following sections we provide a description of the radar electronics and antennas for the VHF and microwave operations (Section 2). For clarity and conciseness, the subsystems developed for the VHF operations will be referred to as the "Radar Depth Sounder" (RDS), while those associated with the 2-8 GHz operations will be referred to as the "Snow Radar" (SR). Section 3 will present results from laboratory testing, and Section 4 will discuss the aircraft integration and ground and flight testing. Conclusions and future work are summarized in Section 5.

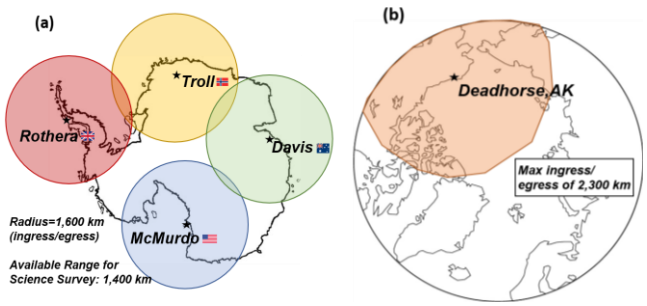

Figure 1: Possible coverage maps for 2-day missions with the Vanilla UAS across the (a) Antarctic (b) Arctic.

2 RECONFIGURABLE SYSTEM OVERVIEW

The Radar Depth Sounder (RDS) is a pulsed radar that operates from 60-80 MHz with a peak transmit power of 200 W per channel and a nominal pulse repetition frequency of 10 kHz. The Snow Radar (SR) is a frequency modulated, continuous wave radar that operates from 2-8 GHz with a maximum transmit power of 1 W. The following sections describe the electronics and antennas for these two operational modes.

2.1 Electronics

The common digital back end uses the HTG-ZRF8 Xilinx Zynq Radio-Frequency System-on-Chip (RFSoC) development platform. This board allows for 8-channel waveform generation and data acquisition with a mixed signal digital processor running embedded Linux. For the reconfigurable radar, the board was configured to support both four transmit and four receive channels for the RDS and one transmitter/receiver pair for the Snow Radar (though currently not simultaneously). Custom firmware was developed to synchronize the waveforms for the 4-channels of the RDS using a multi-tile algorithm.

Due to cabling limitations in the Vanilla UAS wing hard points (discussed later), the RF-subsection of the RDS was split between the chassis and the wing antenna pylons. Figure 2a shows the power conditioning and distribution, power amplifier (PA), transmit/receive (T/R) switch, and low noise amplifier (LNA) modules packaged in the four pylons (additional details are given in [7]). Figure 2b shows the RDS transmit pre-amplifier and variable gain receiver sections packaged in the chassis. As shown in the image, the chassis is pyramidal in shape to fit in the nose cone and contains the digital system, SR chirp generator and transmitter/receiver, and power subsystem. The GPS receiver for data geo-location was also packaged on the back side of the chassis (not visible in Figure 2b).

2.2 Antennas

2.2.1 Radar Depth Sounder

The RDS antenna consists of four dipole elements. Each element is 2.1m long and has a 10-dB return-loss bandwidth of 65-80 MHz. Their locations on the aircraft were determined by the available wing hard points located 1.1 m and 2.2 m from the vehicle center line. The pylon support structure is fabricated from a combination of aluminum and glass fiber reinforced composite materials. The dielectric composite material was necessary to prevent the support structure from shorting out the antenna. The height of the pylon was driven not only by the inclusion of the RF electronics, but proper separation from the aircraft wing. The antenna element must be appropriately spaced from the conductive wing to minimize electromagnetic coupling and disruption of the airflow across the wing.

2.2.2 Snow Radar

The SR antenna, Figure 2c, consists of a custom four-element logarithmically tapered linear monopole array [8]. A Frequency Selective Surface (FSS) is offset from the array 13 mm to improve directivity. The FSS is also visible in Figure 2c along with the dielectric frame that was created to mount the antenna conformally to the vehicle. The array was fed by a 4:1 resistively-loaded power divider. Two sets of arrays were integrated onto the vehicle—one for transmit on the underside of the radar chassis and one for receive in a fiberglass conformal housing installed aft of the landing wheel.

3 LABORATORY TESTS

3.1 Snow Radar Antennas

The two plots in Figure 2c show the measured gain (middle image) and scattering parameter, S_{11}, (bottom image) of the SR antenna conducted in anechoic chambers. As both these plots show, the antenna was designed to operate from 2-18 GHz rather than 2-8 GHz. This design decision was made so that the antenna concept would be compatible with a future Ultra-wideband (UWB) version of the SR. During integration of the antennas, it was found that small manufacturing defects in either the antenna, its feed, or the support structure would cause large dips in the broadside gain over small frequency bands. This was attributed to the slight rotation of the very narrow main beam at some frequencies. While the antenna performance remained satisfactory for the flight test, this is an area of future investigation.

3.2 Transition Board

Only the outer hardpoints of the Vanilla UAS have low-loss RF coaxial cable connections, while both inner and outer hard points are equipped with high-end CAT-6 networking cables (Gore RCN9047-26), which have higher loss and thus limitations in power handling with respect to their coaxial counterparts. While not ideal, this installation restriction was the driving factor for integrating critical parts of the RF electronics into the wing pylon. A custom “transition board” was thus developed to pass RF signals through the 100-Ohm twisted pairs available in wings of the aircraft. Figure 3a is an early prototype of the transition board that included a set of impedance transformers to convert the 100-Ohm differential cable impedance into 50-Ohms (single-ended). Prototype

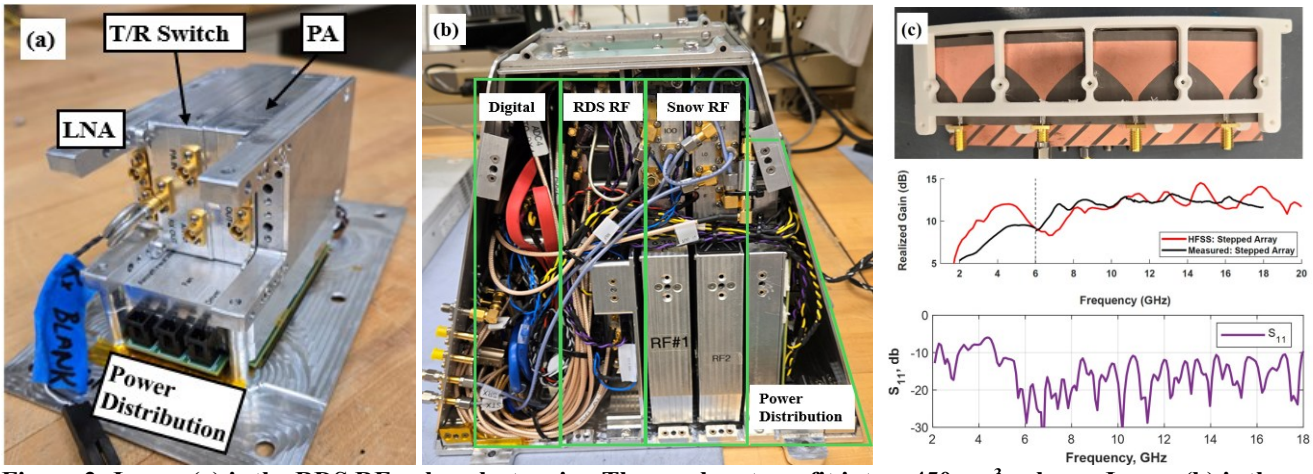

Figure 2: Image (a) is the RDS RF pylon electronics. These subsystems fit into a 450 cm^3 volume. Image (b) is the radar chassis with RF, digital, and power submodules. The top image in (c) shows the 4-element conformal SR monopole array. The FSS can be seen sticking out on the bottom of this image. The plot in the middle of (c) is the gain measurement, while the bottom image is the S_{11}.

testing indicated an insertion loss (including transformers) of ~2 dB (inferred from $|S_{21}|$ in Figure 3c) for a 4.8 m run and an isolation between pairs of >40 dB (not shown in the plot).

3.3 Delay Line Tests

Prior to fielding the system, both radar modes (RDS and SR) were tested using a fiber optic delay line and RF attenuators. Figure 4a shows representative delay line result for a single channel of the RDS system (the ~34 µs delay was confirmed with an independent network analyzer measurement). A similar test was conducted with the SR using a 1.754 µs delay line and attenuators (Figure 4b).

4. AIRCRAFT INTEGRATION AND FLIGHT TEST

Figure 5a and b show the fully installed system on the vehicle. Figure 5a was taken during flight, and the four VHF dipole antennas are clearly visible. The aft SR antenna is also highlighted in the image. While not visible in Figure 5b, the forward SR antenna was installed on the bottom of the radar chassis. In the foreground of Figure 5b is the radar-mounted transition board that takes the output RF signal from the radar and passes it to the network cable. The total weight of the radar electronics and chassis was 8 kg, while each pylon antenna and the installed VHF electronics were 2.7 kg and 0.25 kg, respectively

During ground testing of the system the basic functionality of the system was established and the insertion losses of the vehicle's network cables combined with the final transition boards were confirmed to be in the 1.4-2.6 dB range for 60-80 MHz; however, during the ground engine test an intermittent, strong, narrowband Radio Frequency Interference (RFI) signal of unknown origin was observed on the RDS radar at ~ 65.7 MHz. This interference only showed up while the engine was running and the signal increased with engine RPM and we have not been able to reproduce it in the laboratory. While the exact source of this issue is still being investigated, it was rarely observed during flight. This

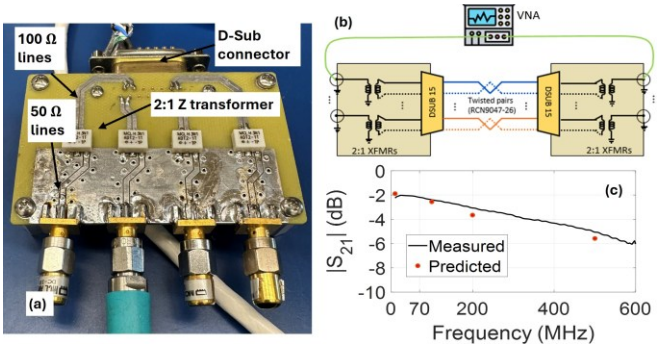

Figure 3: Inset (a) is the prototype board, while (b) shows the test setup. Inset (c) shows the measured insertion loss.

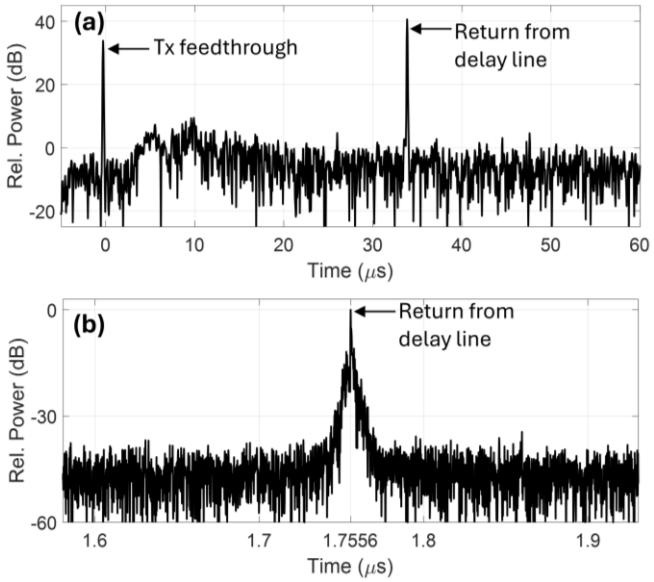

Figure 4: Delay line measurements conducted in the laboratory for the RDS system (a) and Snow Radar (b).

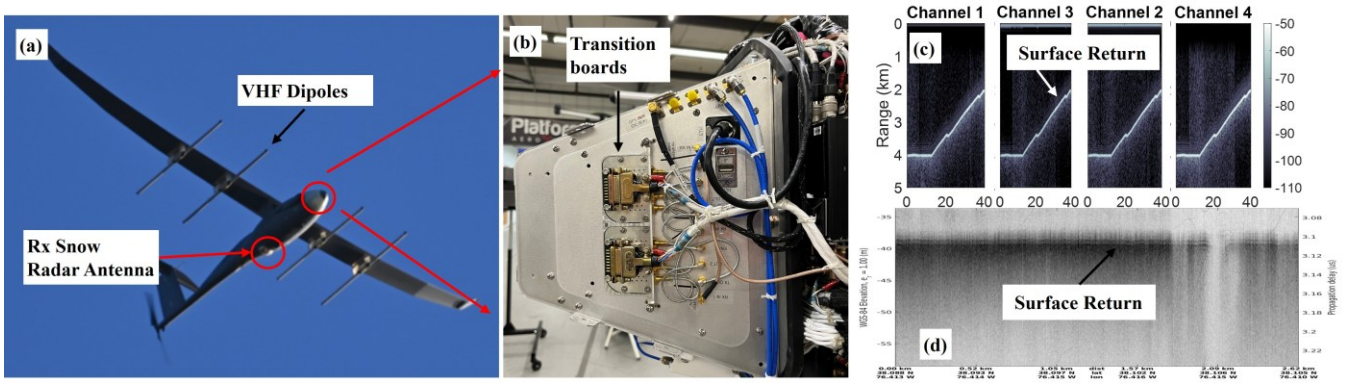

Figure 5: Image (a) shows instrumented vehicle in flight during the test. The radar chassis installed in the nose is shown in (b). Image (c) and (d) show the surface returns from the RDS and SR measured during the flight test. The x-axis in (c) is distance (km). On the rights side of (d), the image appears to fade due to vehicle banking during a turn.

suggests that the cause of the RFI may be related to the mechanical vibrations of the airframe. The severity of the vibrations was much more significant during a ground test due to the vehicle being restrained. Overall, the presence of the RFI did not affect the system performance during flight.

System flight test was based out of Webster Field in Virginia and completed on 2 November 2024. The vehicle flew a racetrack pattern over the Potomac River, ascending to an altitude 4,100 m above ground level (AGL) over the course of 2.5 hours. The total flight time was just over 4 hours. The RDS was turned on via a remote connection and began recording data when the vehicle reached a flight altitude of 760 m. The RDS was operated with a reduced bandwidth of 75-80 MHz, primarily due to the frequency approval granted by the Federal Communications Commission (FCC) for the flight test. To prevent uncorrected cable delay offsets causing transmit beam pattern distortion, we operated exercising a single transmit channel and four receivers. However, the digital system is capable of amplitude/time/phase adjustments on a per-channel basis, and future flights will include a transmit equalization routine as done in [9]. The gain for the four receivers was set well below the saturation point for strong surface returns at the lowest planned flight altitude for both transmit waveforms. For the latter we used a combination of 1-µs and 10-µs long pulses with 8 and 16 onboard presums, respectively. Just over 1 hour, or 340 GB, of data (85 GB/channel) were recorded. During the flight, the radar sent back periodic, small data packets so the performance could be monitored in real-time. We observed comparable performance across channels. After the vehicle descended to 500 m the RDS radar was turned off, and the SR was turned on which subsequently collected a total of 4 GB of data.

Figure 5c and d show the surface returns collected by the RDS and SR, respectively. The radar returns on the first ~12.5 km of the frame were collected at a levelled altitude of ~4 km (~13,120 ft) above the water surface, after which the gradual aircraft descent is apparent from the echogram. The SNR obtained during the levelled flight with the 10-us waveform and additional coherent integrations, was ~55-60 dB. In the SR echogram (Figure 5d), the weaker surface return at 70% frame length (~1.8 km from the start) is due the vehicle banking in a turn, and the antenna main beam momentarily not pointing towards nadir before the acquisition stopped. The SNR of the surface return for the processed SR data was ~40 dB. The range sidelobes can be reduced through a deconvolution to correct systematic effects, as shown in [10].

5. CONCLUSIONS AND FUTURE WORK

Overall, the integration and flight test of the reconfigurable radar on the Vanilla UAS was successful. Both modes of operation performed as expected; however, several areas of improvement have been identified and discussed in the paper.

We are currently preparing the system to be installed on the Windracers ULTRA UAS as part of a collaboration with the Norwegian Polar Institute (NPI) and the Norwegian Research Centre (NORCE). For this installation, the RF electronics that were installed in the pylon for the Vanilla are packaged in a different unit and installed next to the rest of the radar electronics. As such, the pylons were reduced in height. Initial ground tests were completed earlier this year, and flight tests will follow in the second half of 2025. The first Antarctic survey campaign is scheduled for the 2025/2026 Austral Summer season.

ACKNOWLEDGEMENTS

We gratefully acknowledge funding from the U.S. National Science Foundation, NSF (Award# 2216455). We also thank our collaborators at Platform Aerospace; J. Laverentz for logistics/programmatic support; A. Paden, W. Goble, B. Schroeder for fabrication, J. Barnhill, A. Sethi, B. Peek, B. Mura, C. Lindsey, S. McMillan, and other students for design and test support.

REFERENCES

[1] U.S. Army, "U.S. Army Roadmap for UAS 2010-2035," https://fas.org/irp/program/collect/uas-army.pdf. Retrieved 1/14/2025.

[2] Mersmann, K., “NASA is Helping Fly Drones in the Arctic. Here’s What That Means for Sea Ice and Sea Level Change,” https://www.nasa.gov/earth-and-climate/nasa-is-helping-fly-drones-in-the-arctic-heres-what-that-means-for-sea-ice-and-sea-level-change/. Accessed 17 Jan. 2025.
[3] Arnold, E.J., A. Patil, F. Rodriguez-Morales, V. Occhiogrosso, “Near-HF Electrically Small Antenna for UAS Ice-Penetrating Radar,” *Microwaves and Optical Technology Letters,* March 2022. DOI: 10.1002/mop.33225.
[4] Rose, G., E. Arnold, J. Paden, F. Rodriguez-Morales, C. Leuschen, D. Gomez-Garcia, “Ice-Bed Detection Capabilities of a Low-VHF Radar on a Small UAS,” *IEEE Aerospace Conference 2025*, *Big Sky, MT*. Accepted.
[5] Teisberg, T. "Seeing Secrets in the Ice: A Drone-Based Radar Looks for the Future of Climate Change." *IEEE Spectrum,* Vol. 60, No.10, Aug. 2023, pp. 22-29.
[6] Teisberg, T.O., D. M. Schroeder, A. L. Broome, F. Lurie and D. Woo, "Development of a UAV-Borne Pulsed ICE-Penetrating Radar System," *IGARSS 2022 - 2022 IEEE International Geoscience and Remote Sensing Symposium*, Kuala Lumpur, Malaysia, 2022, pp. 7405-7408, doi: 10.1109/IGARSS46834.2022.9883583.
[7] J. Barnhill, W. Fischer, C. Lindsey, S. McMillan, B. Mura, B. Peek, M. Rahman, A. Sethi, E. Arnold, D. Gomez-Garcia, S. Kaundinya, C. Leuschen, J. Li, and F. Rodriguez-Morales, Development and Flight Tests of Wing-Mounted T/R Modules for a UAS-borne Multichannel VHF Ice Penetrating Radar, *Proc. IEEE Texas Symp. Wireless Microw. Cir. Syst.*, Waco, TX, April 2025
[8] C. Hilton, J. Nanzer and J. Papapolymerou: "UWB antenna element on conformal substrate for S-Ku band applications" presented at the 2024 IEEE International Symposium on Antennas and Propagation, July 2024, Florence, Italy.
[9] Yan, J., et al., “Meas. of in-flight cross-track antenna patterns of radar depth sounder/imager,” IEEE Trans. Antennas Propag., vol. 60, no. 12, pp. 5669–5678, 2012.
[10] C. Leuschen, R. Forsberg, E. Arnold, Stokholm, T. Jensen, J. Li, J. Paden and F. Rodriguez-Morales, Dual-Frequency Radar Measurements for the SWIDA-RINGS Mission: Circumventing Antarctica to Map Its Grounding Line, *IEEE Int. Geosci. Remote Sens. Symp.,* Brisbane, Australia, 2025, Aug. 2025.